[^{99m}Tc]Tc-HYNIC- EcgDf21 a defensin short analog with potential application in infection foci imaging.

Mariella Terán[1], Jessica Osorio[1], Elena Cardoso[1], Emilia Tejería[1], Andrea Paolino[3], Ana Laura Reyes[3] and Gianna Cecchetto[2]

1 Área de Radioquímica, Departamento Estrella Campos, Facultad de Química, Universidad de la República (Udelar), Montevideo, Uruguay.
2 Área de Microbiología, Instituto de Química Biológica, Facultad de Ciencias-Departamento de Biociencias, Facultad de Química, Universidad de la República (Udelar), Montevideo, Uruguay.
3 Centro Uruguayo de Imagenología Molecular (CUDIM), 11600 Montevideo, Uruguay

* Dr. Mariella Terán; 0000-0003-4566-0814
General Flores 2124, 11800, Montevideo,Uruguay.
E-mail: mterangretter@gmail.com

Abstract:

Short running title:

[^{99m}Tc]Tc-HYNIC- EcgDf21 for infection foci imaging

Opportunistic infections are a problem of great relevance in public health and the precise detection and localization of infection in the early stages of the disease is of great importance for patient management as well as cost containment. Our proposal seeks to contribute to developing a new agent that meets the needs of diagnosis and follow-up of fungal and bacterial infections, focused on the design of a radiotracer with the potential for recognition of hidden infection foci. Defensins, are plant antimicrobial peptides that, not only show activity against plant pathogens but also against human ones. A short analog of EcgDf1 defensin, EcgDf21d (NH_2-ERFTGGHCRGFRRRCFCTKHC-COOH), was labelled through the formation of a ^{99m}Tc-HYNIC complex which was assessed for physicochemical and biological behaviour both *in vitro* and *in vivo*.
The [^{99m}Tc]Tc-HYNIC- EcgDf21 labelling procedure rendered a single product with remarkably high RCP and stability in the labelling milieu. The Log P value indicated that [^{99m}Tc]Tc-HYNIC-EcgDf21 has a hydrophilic behaviour, confirmed by the biodistribution profiles. The optimal uptake value was obtained for *C. albicans* infection model reaching a lesion/muscle ratio of 3, this correlates with *in vitro* binding studies, and the lesion can be definitely observed in the scintigraphic images.

Introduction

Opportunistic infections are a problem of great relevance not only for patients but also for physicians who must manage the disease. Within the more recurrent nosocomial bacterial species are *Staphylococcus aureus*, *Pseudomonas aeruginosa,* and *Klebsiella pneumoniae*, while invasive fungal infections have been characterized mainly due to the presence of species such as *Candida* spp. and *Aspergillus* spp. Precise and early diagnosis of infectious focus can be difficult and time-consuming due to the diversity and changing spectrum of micro-organisms (m.o) that can cause disease. Therefore, accurate detection and localization of infection and inflammation foci in the early stages of the disease is of great importance for patient management as well as cost containment (Lucignani, 2007). For such goals, Nuclear Medicine is a valuable tool that uses radioactive compounds (radiopharmaceuticals) for diagnostic purposes consisting of systemically administering a radioactive gamma emitter tracer, whose radiation of high penetrating power can be detected externally (Jain, 2017; Ordonez, 2019; Signore, 2020). This allows for evaluating the functionality of the organs and the biochemistry of the lesions in a non-invasive way to detect alterations associated with various diseases. Many radiopharmaceuticals have been developed as diagnostic agents for Nuclear Medicine such as antibiotics, cytokines, leukocytes and antimicrobial peptides. During the last years, compounds derived from human antimicrobial peptides such as ubiciquidin (Welling, 2004; Meléndez-Alafort, 2009), lactoferrin (Brouwer, 2011), and human neutrophil α, β-defensins, among others, have been assessed as potential radiotracers for detection of infections. Particularly, the successful development of ^{99m}Tc-UBI (29-41) and ^{68}Ga-UBI(29-41) (Vilche, 2016) as radiopharmaceuticals, stimulated the exploration of new antimicrobial peptides (AMPs) derived from different sources. In this sense, our group focused its interest on defensins, which constitute the largest family of AMPs, components of plant innate immunity and are considered non-toxic to plant and mammalian cells (Zasloff, 2002; Thevissen, 2004). These AMPs have compact tertiary structures stabilized by disulfide bonds between highly conserved cysteines, they are small in size, have positive general charge, amphipathic stereogeometry, and broad biological activity, these characteristics make them resistant to variations in pH and temperature. Its cationic nature under physiological conditions, associated with tendency to adopt amphipathic structures would facilitate their interaction and insertion within the walls negative cell and phospholipid membranes of microorganisms. The characteristics described above and the fact that defensins, like other plant AMPs, not only show activity against plant pathogens but also against human ones, have generated great interest in these compounds for the development of new drugs with antibiotic action and as agents for the diagnosis and prevention of infections (Kovaleva, 2020; dos Santos, 2020, Ishaq, 2019; de Oliveira Carvalho, 2011). In this line, our proposal seeks to contribute to developing new agents that meet the needs of diagnosis and follow-up of fungal and bacterial infections, focused on the design of new radiotracers with the potential for recognition of hidden infection foci (Muammad, 2012). For this purpose, we selected a short analog of defensin from the native plant Ceibo, *Erythrina crista-galli*, EcgDf1 (Rodriguez-Decuadro, 2019), which inhibits the growth of

microorganisms of interest such as *Candida* spp and *Aspergillus* spp (Figure 1).

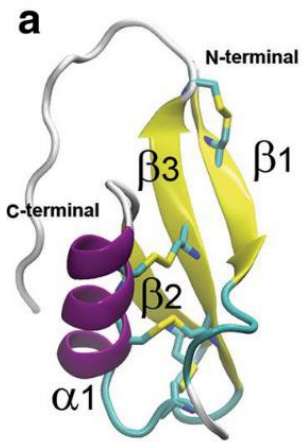

Figure 1: Structure of EcgDf1 defensin (ERFTGGHCRGFRRRCFCTKHC) (Rodríguez-Decuadro. S, 2019)

In order to choose the radionuclide to label the defensin, we selected technetium-99m which continues to occupy a prominent place in diagnostic nuclear medicine mainly due to its wide availability and low cost. As a transition metal, it has rich coordination chemistry which offers many possibilities of oxidation states, cores, and electron donor groups. Labelling biologically active molecules with tecnetiumn-99m by the formation of a coordination compound faces an inherent difficulty since it is necessary to develop adequate methods that allow binding the ligand to the metal without altering the biological activity of the molecule of interest (Tehrani, 2021). Our group has been working extensively in the development of radiotracers for infection detection by scintigraphic images based on antibiotics, antifungals, and phages as potential agents using technetium-99m through different radiolabelling approaches (Cardoso, 2016; Fernández, 2017; Reyes,2014; Terán, 2012). Based on that experience we chose among the multiple strategies available for the radiolabeling of biomolecules one of the most extended methods, the Bifunctional Chelating Agent (BFCA) approach. This involves the conjugation of a peptide or protein with a BFCA and the subsequent formation of a coordination complex with tecnetiumn-99m. One of the most popular and effective BFCA is HYNIC (6-hydrazinonicotinamide) (Abrams, 1990). Which is commonly linked to biomolecules through an amide bond formed by the reaction of amine side chains in the biomolecule with an active ester such as N-hydroxysuccinimide (NHS). This makes possible the union of the BFCA to the peptide at a remote location from the biologically active site. In this way, adding a metallic element will not alter the biochemical properties of the peptide. The use of HYNIC requires an additional ligand, such as tricine to complete the technetium coordination sphere, the proposed structure of the complex is shown in Figure 2.

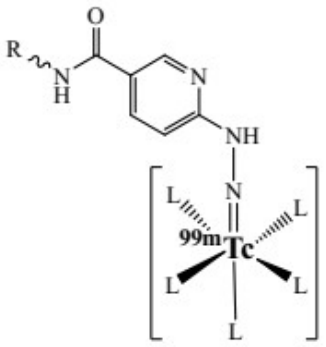

Figure 2 : Proposed complex structure R= defensin EcgDf1, L =tricine ligand

Taking all the above into consideration, we present herein the preparation and evaluation of the ^{99m}Tc-labeled defensin short analog EcgDf21d with potential application in infection foci imaging. Labelling was performed through the preparation of HYNIC-tricine technetium complex. The biologically active amino acid sequence of EcgDf1 defensin (NH_2-ERFTGGHCRGFRRRCFCTKHC-COOH) has its active core in the acid terminal end, so, the peptide was derivatized in the amino terminal group (E) with HYNIC and the coordination sphere of the complex was completed with tricine. The final ^{99m}Tc-complex was assessed for physicochemical and biological behaviour both *in vitro* and *in vivo* against *Candida albicans*, *Aspergillus niger,* and *Staphylococcus aureus*.

Results and Discussion

Radiolabelling

The short synthetic analog of defensin EcgDf21 (ERFTGGHCRGFRRRCFCTKHC) containing 21 amino acids was derivatized on the N terminus with HYNIC as a chelator for technetium-99m, through an amide bond. According to the literature, this amino acid sequence is responsible for the biological activity and the modifications reported enhance selectivity and stability (Rodriguez-Decuadro, 2019)
Different labelling conditions were assessed such as peptide mass (30, 50, 100 µg), incubation temperature (room temperature 20ºC, 70ºC, and 95°C), and reaction time (5, 15, and 30 minutes) at pH 4.5. Radiochemical purity (RCP) was determined by HPLC and TLC as described in the experimental section. The results using different radiolabelling conditions are summarized in Table 1.

Table 1: Radiochemical purities (RCP%) of [^{99m}Tc]Tc-HYNIC-EcgDf21 achieved using different labelling conditions (n=3 ±SD)

Peptide mass (µg)		
30	50	100
RCP%		
98.0± 3.1	95.3± 4.8	87.7±5.5

Incubation temperature (ºC)		
20	70	95
RCP%		
18±4.3	88.1±5.0	98±4.7

Incubation time (min)		
5	15	30
RCP%		
71±6.8	87±6.1	98±3.5

According to these results, the best radiolabelling conditions to obtain the peptide complex, from now on [^{99m}Tc]Tc-HYNIC-EcgDf21 were: 30 µg of ligand, pH 4.5, incubation temperature 95ºC during 30 minutes. HPLC analysis shown in Figure 3 revealed the formation of a single product with a retention time (*rt*) of 9,7 min with a RCP higher than 95%. Paper chromatography did not reveal the presence of [^{99m}Tc]TcO_4^-, and the amount of [^{99m}Tc]TcO_2 was 6,3 ± 0,31 %

The [^{99m}Tc]Tc-HYNIC- EcgDf21 was obtained with a specific activity of 1,2MBq/µg.

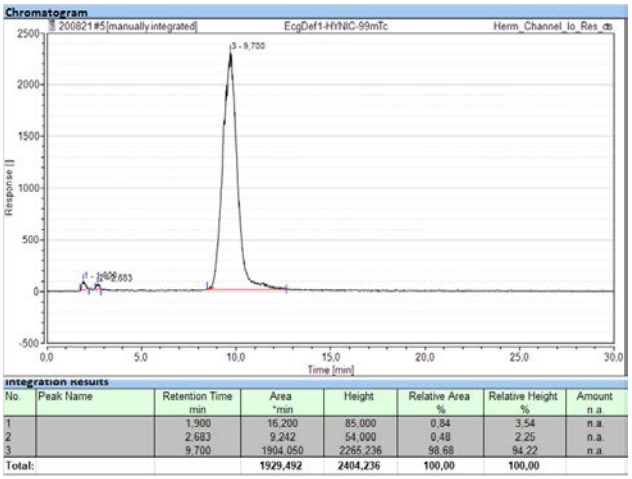

Figure 3: High-performance liquid chromatography profile of [^{99m}Tc]Tc-HYNIC-EcgDf21 using 30 µg of ligand, pH 4.5, incubation temperature 95ºC during 30 minutes.

Physicochemical evaluation

In order to assess the potentiality as radiopharmaceutical of the complex [^{99m}Tc]Tc-HYNIC-EcgDf21, the main physicochemical properties of the radiolabelled peptide were determined namely stability, lipophilicity, and plasma protein binding.

Stability in labelling milieu, in human plasma and after incubation with cysteine as competitive ligand was assessed by HPLC and TLC.

The complex was stable in the labelling milieu for at least 4 hours with RCP higher than 95% and after incubation. Nevertheless, it decomposed after 1 hour of incubation in human plasma indicating a possible enzymatic degradation.

Stability against ligand exchange was studied by incubating with a 5-fold molar excess of cysteine for two hours. This amino acid, usually present in plasma proteins, is an excellent competitive agent to bind technetium. [^{99m}Tc]Tc-HYNIC- EcgDf21 presented slight exchange of ligands after 2 hours of incubation, indicating chemical stability under stress conditions.

Lipophilicity was assessed through the determination of the partition coefficient between 1-octanol and phosphate buffer 0.1M pH 7.4. [^{99m}Tc]Tc-HYNIC- EcgDf21 was hydrophilic, with a Log P of (-0.60 ± 0.01).

Plasmatic protein binding (PPB) was assessed by size exclusion chromatography at 0.5 and 1 hour. The complex showed moderate PPB, which is a positive property for potential radiopharmaceuticals since only the unbound fraction of [^{99m}Tc]Tc-HYNIC-EcgDf21 can bind to microorganism membranes. The physicochemical results are summarized in Table 2.

Table 2: Log P, PPB, and ligand exchange results at 0.5 and 1 hour (n=3 ±SD).

Log P	PPB (%)		Ligand exchange (RCP%)		
	0.5 h	1 h	0.5 h	1 h	2 h
-0.60 ± 0.01	44.4 ± 6.3	49.9 ± 6.7	94.0 ± 2.2	92.0 ± 3.5	88.1±3.1

Biological evaluation

***In vitro* studies**

The bacterial and fungi binding assay showed a clear increase in activity retained in the pellet at higher concentrations of m.o cells. Consequently, a plateau in the curve indicates saturation of the complex-m.o interaction. For *Candida albicans*, the binding percentage reached a maximum of 98.75 ± 2.03, for *Aspergillus niger* 81.04 ± 5.9 and for *Staphylococcus aureus* 96.34 ± 3.1, as shown in Figure 4.

a)

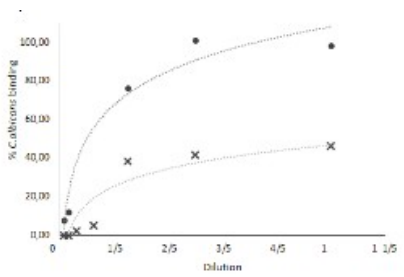

b)

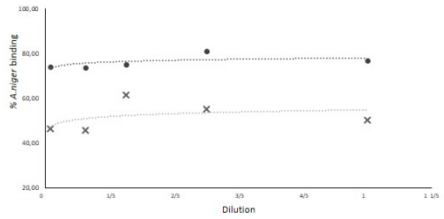

c)

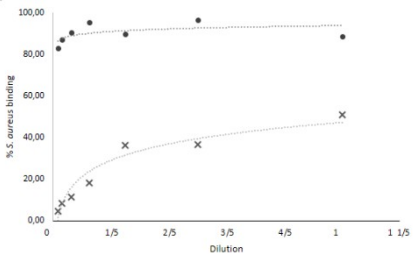

Figure 4: Binding profile of [^{99m}Tc]Tc-HYNIC-EcgDf21 with m.o cultures a) *C. albicans,* b) *A. niger* and c) *S. aureus*. The percentage of radio-labelled complex retained versus concentration of m.o is plotted. Full dots: non-blocked; crosses: blocked with non-radiolabelled ligand.

For all three samples of m.o, the [^{99m}Tc]Tc-HYNIC-EcgDf21 binding profiles were significantly reduced by competition with the non-radioactive ligand HYNIC-EcgDf21 resulting in a decrease in uptake of approximately 45%, as shown in Figure 4. This indicates the specificity of radiotracer-microorganism binding.

***In vivo* studies**

Biological evaluation of [^{99m}Tc]Tc-HYNIC-EcgDf21 was performed in normal mice (G1) in order to determine the biological distribution of the complex, with special attention on blood pharmacokinetics behaviour, routes of elimination, and accumulation sites. Figure 5 shows biodistribution values of Injected Dose percentage (% ID) of the biological models at 2 hours post administration of the complex.

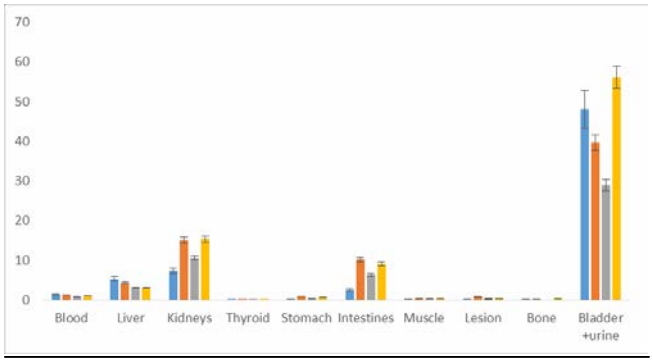

Figure 5: Biodistribution profile of all the biological models at 2 hours post injection of [^{99m}Tc]Tc-HYNIC- EcgDf21. (n=3 ± SD)

The collective accumulation stomach and thyroid of [^{99m}Tc]Tc-HYNIC-EcgDf21 was low, indicating that no *in vivo* reoxidation occurs. The highest accumulation organs are kidneys with an average of 15% ID uptake, independently of the biological model. The complex is eliminated mainly by urinary path, 55% ID, in accordance with its Log P value.

The uptake of the complex in the induced lesions (L) and the normal muscle (M) was quantified by measuring samples both during biodistributions (BD) and image quantification for all the groups.

The ratio L/M is shown in table 3, the results between both calculation methods did not show a statistically significant difference (Unpaired T test p value < 0.05 GraphPad Prism version 6 (GraphPad Software, San Diego, CA, USA) except for G3.

Table 3: Lesion (L) to muscle (M) ratio (n=3 ± SD)

L/M ratio	G1 LPS	G2 C.albicans	G3 A.niger	G4 S.aureus
Biodistribution	1.37±0.90	2.7±0.35	0.85 ±0.15	1.31±0.42
Image quantification	1.02±0.02	2.91±0.14	1.7±0.5	1.35±0.6

Despite the high binding values of [^{99m}Tc]Tc-HYNIC-EcgDf21 to *in vitro* microorganism cultures, the *in vivo* uptake in animals was only remarkable in G2, *C. albicans*, having almost three times more activity in the lesion than in the normal muscle. Group 3 corresponding to *A. niger* showed slight uptake in scintigraphic images but this behaviour was not confirmed by biodistribution. This difference may be due to the infection foci characteristics that are usually diffuse and difficult to separate from the muscle during dissection, but can be focused in the SPECT image. In the case of G4, both quantification methods led to similar results but there was no significant difference in uptake when compared with G1 *LPS* sterile inflammation.

Figure 6 shows the scintigraphic images corresponding to animals of G2, G3 and G4.

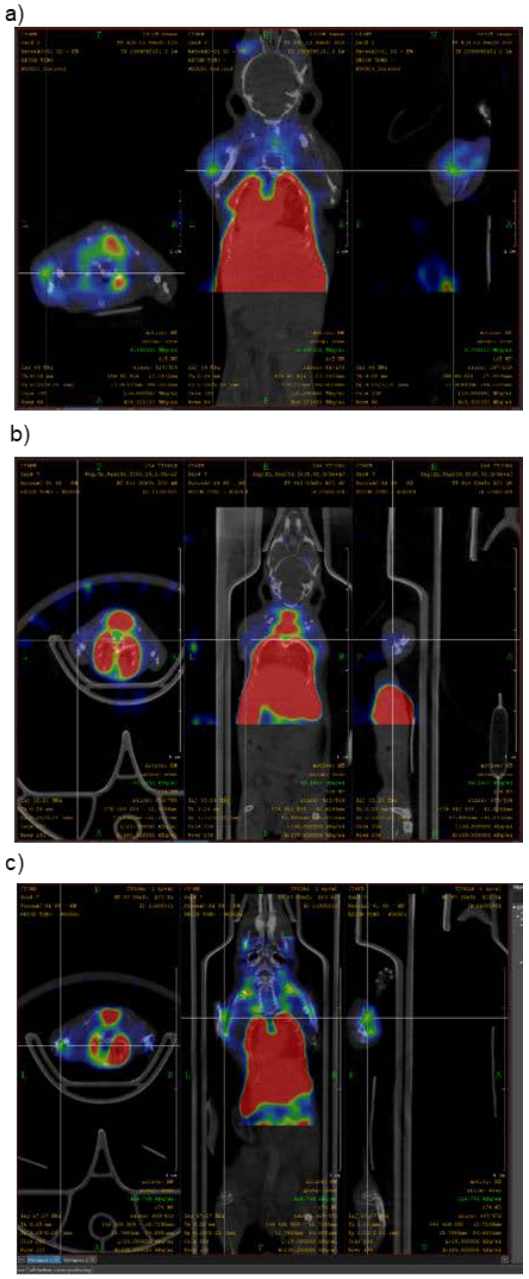

Figure 6: Scintigraphic images of [^{99m}Tc]Tc-HYNIC- EcgDf21 in Balb. C mice infected a) *C. albicans,* b) *A. niger* and c) *S. aureus*

Conclusions

In the present work, we described the development, *in vitro* and *in vivo* evaluation of a new radiolabelled antimicrobial peptide EcgDf21, obtained by preparation of a ^{99m}Tc HYNIC complex. The labelling approach is very simple because the BFCA moiety can be easily added to the peptide and this ligand can be maintained in freezer for several weeks. Furthermore, the labelling procedure rendered a single product with remarkably high RCP and stability in labelling milieu.

Physicochemical evaluation showed that the [^{99m}Tc]Tc-HYNIC-EcgDf21 complex has adequate properties including high stability in milieu and against cysteine maintaining high RCP during the time of observation that represents the time needed for biological evaluation. The challenge against human plasma suggested that the complex may suffer enzymatic degradation *in vivo*.

In vitro studies of binding to m.o cultures, showed that [^{99m}Tc]Tc-HYNIC- EcgDf21 maintains its capability of interacting with the pathogens assessed at several dilutions, being all above 70% at least at the 1/5 dilution. This is a good indicator that the peptide remains biologically viable despite de chemical modifications derived from the radiolabelling process. Complementary competition studies confirmed the specific binding of the [^{99m}Tc]Tc-HYNIC-EcgDf21 to m.o showing a marked decrease when incubated with the competing non-radiolabelled ligand.

Regarding biological evaluation in animal models, the biodistribution profile for both sham and injured groups revealed that the complex does not suffer *in vivo* reoxidation of ^{99m}Tc as the %ID in stomach and thyroid are negligible, these results are in accordance with the physicochemical studies that indicate chemical stability in time and against cysteine. The Log P value indicates that [^{99m}Tc]Tc-HYNIC-EcgDf21 has a hydrophilic behaviour which is confirmed by the biodistributions, where a mean of 55% of the injected dose is eliminated by urine.

As the objective of this work was to develop and evaluate a potential radiotracer for infection foci, the uptake in induced lesions, both by m.o or sterile inflammation was crucial. One of the characteristics required for this kind of compounds is its ability to discriminate between infection and inflammation, the model of sterile inflammation represented by G1, LPS showed no interaction with [^{99m}Tc]Tc-HYNIC-EcgDf21, this was confirmed both through biological samples (L/M= 1.02±0.02) and image quantification. In the case of G4 (*S. aureus*), the uptake value was similar to G1, 1.02±0.2, and 1.3±0.6 respectively, despite the good profile obtained *in vitro* with this culture. This behaviour can be explained by the characteristics of the *S. aureus* infection which forms a membrane that encapsulates the foci, preventing the penetration of the complex.

G3 (*A. niger*) presented a low L/M ratio although it is statistically different from the profile shown by G1 and G4 it is not good enough to clearly discriminate the lesion. The optimal value was obtained for the *C. albicans* model reaching an L/M ratio of 3, this correlates with *in vitro* binding studies, and the lesion can be definitely observed in the scintigraphic images.

Lesion uptakes are modest in comparison with other radiolabelled peptides cited in bibliography, for example [^{99m}Tc]Tc-HYNIC-UBI29-41 presented accumulation in infected tissues with L/NT ratios of 2–3, and no accumulation in tissues with inflammation (Gandomkar,2009). ^{99m}Tc-labeled synthetic fragment of human lactoferrin (hLF1–11) showed a T/NT ratio of 3.5 to 4 in animal models of infection (Browner, 2008). Human β-defensin 3 (HBD-3) was labelled and the complex ^{99m}Tc-labeled HBD-3 was able to discriminate *S. aureus* infection from sterile inflammation with T/NT of 5.7 (Follacchio, 2019).

In this work, the development of a new radiolabelled antimicrobial peptide for infection imaging was achieved. [^{99m}Tc]Tc-HYNIC-EcgDf21 showed adequate *in vitro* behaviour and preclinical studies revealed that the peptide structure can differentiate between sterile inflammation and infection in *C.albicans* lesions. Nevertheless, the other infections could not be clearly discriminated *in vivo* despite having very good *in vitro* binding profiles. The general pharmacokinetic behaviour makes this a

basic structure worthy to deepen its study. Slight modifications to the peptide sequence are currently being studied in order to improve the in vivo behaviour and image performance.

Experimental Section

Materials

[^{99m}Tc]TcNaTcO4 was obtained from a commercial [^{99}Mo]Mo/[^{99m}Tc]Tc generator (Tecnonuclear, Argentina). All laboratory chemicals were reagent grade and were used without further purification. HYNIC, L-cysteine, Tricine, $SnCl_2.2H_2O$, bovine serum albumin (BSA) and trifluoroacetic acid (TFA) were purchased from Sigma-Aldrich. Solvents for chromatographic analysis were HPLC grade.

The peptide of sequence EFTGGHCRGFRRRCFCTKHC (PM: 2558) was synthesized by NovoPro Bioscience. Inc (China) with purity higher than 90%, analysed by reverse phase HPLC (RP-HPLC) and MS.

Activity measurements were performed either with a dose calibrator (Capintec CRC-5R) or with a scintillation counter (3×3'). NaI (Tl) crystal detector) attached to an ORTEC monochannel analyser. Paper radiochromatography was carried out on Whatman 1 support and scanned with a radiochromatograph EZ-SCAN Carroll & Associates, SRI – model 302.

HPLC analysis was carried out on Thermo Scientific UltiMate 3000 using a reverse phase column (Waters DeltaPak (150 x 3.9mm C18 5µm, 300Å). Elution was performed at 1.0 mL/min flow rate with a binary gradient system of 0.1% trifluoroacetic acid in water as mobile phase(A) and 0.1% trifluoroacetic acid in acetonitrile as mobile phase (B). The elution profile was as follows: 2-5 min 2% B, 5-10 min 2-50% B, 10-20 min 50% B, 20-25 min 50-70% B. Detection was accomplished with a 1"x1"NaI (Tl) crystal scintillation detector (Xiangli Liu et al, 2011)

Conjugation of EcgDf21with HYNIC

650 µg NHS-HYNIC dissolved in 325 µL DMSO was slowly added to 2 mL solution of peptide and incubated in darkness for 30 minutes. This solution was purified by Sep-Pak C18 Cartridge to remove non-bound HYNIC. EcgDf21-HYNIC solution was stored at -20°C under N2 atmosphere until use.

Preparation of [^{99m}Tc]Tc-HYNIC- EcgDf21 complex

The labelling process consisted of the preparation of two solutions namely: the conjugated peptide EcgDf21-HYNIC, 1 mg/mL, (A), and the coligand and reducing agent containing 0,3 mg/mL of Tricine and 1.1 mg/mL of SnCl2 (final pH= 4.5), (B).

An aliquot of 30 µL of solution A was added to 30 µL of B. After homogenization, 100µL of [^{99m}Tc]NaTcO4 (37 MBq/mL,1mCi/mL) were added and incubated during 30 minutes at 95°C. Radiochemical purity of the complex (RCP) was assessed by reverse phase HPLC. The presence of free [^{99m}Tc]TcO4- was determined by chromatography in Whatman1 as stationary phase and NaCl 0.9% as mobile phase (Rf=1) measured in a radiochromatograph scanner Scan-Ram (LabLogic). [^{99m}Tc]TcO2 (colloid) was determined by measuring the retained activity in the HPLC column.

***In vitro* evaluation**

Stability in labelling milieu

[^{99m}Tc]Tc-HYNIC-EcgDf21 was incubated in the labelling milieu at room temperature for 0.5, 1, 2, and 4-hours post labelling and the RCP was assessed using the reference system mentioned above.

Stability in plasma

In vitro stability was assessed by incubating the complex (200 µL) with fresh human plasma (1000 µL) at 37°C. Samples of 150 µL were collected at 0.5 and 1 hour and precipitated with 150 µL of cold absolute ethanol (-15°C) and cooled in a freezer for 5 minutes to induce precipitation. After centrifugation at 156 g for 5 min at 0ºC, the pellet was carefully separated from the supernatant and an aliquot of the latter was analysed by HPLC with the reference system.

Stability in the presence of competing ligands

A sample of [^{99m}Tc]Tc-HYNIC-EcgDf21 (200 µL) was incubated with 1000 µL of a solution of 5 molar excess of L-cysteine at 37°C. RCP was determined after 0.5, 1, 2 and 3 hours by HPLC analysis as described above. (Von Guggenberg, 2004)

Lipophilicity

Lipophilicity was determined as the partition coefficient of 1-octanol/phosphate buffer (0.1M, pH 7.4) (Goodman&Gilman, 2007). In a centrifuge tube, 2 mL of 1-octanol and 2 mL of phosphate buffer 0.1 M pH 7.4 were mixed. 100 µL of complex were added and shaken on a vortex mixer for 2 minutes. The mixture was centrifuged for 5 minutes at 1113 g; an aliquot of each phase (n=2) was measured in a solid scintillation counter. Partition coefficient (P) was calculated as the mean activity value of the organic phase divided by the aqueous one; lipophilicity was expressed as log P (Trejtnar, 2002).

Protein binding (PPB)

Binding to plasma proteins was determined by size exclusion chromatography. The complex (50 µL) was incubated with fresh human plasma (450 µL) at 37ºC up to 1 hour. At 30 and 60 minutes, 25 µL samples were seeded in a size-exclusion chromatography column (Microspin G-50, GE Healthcare, Buckinghamshire, UK). Columns were centrifuged at 1113 g for 1 minute and activity of the eluate and the column was measured in a solid scintillation counter.

The PPB% was calculated as:

$$(net\ activity\ eluted / total\ activity) x 100$$

being total activity (eluted + retained in the column) (n = 3).

***In vitro* microbiological studies**

To evaluate the capacity of the complex to bind to different pathogenic m.o *C. albicans* ATCC 101231 (yeast), *A. niger* CCMG17 (filamentous fungus, Cátedra de Microbiología General Collection CCMG, Facultad de Química, Montevideo, Uruguay) and *S. aureus* ATCC 25923 (Gram positive bacteria) were selected. *C. albicans* and *S. aureus* concentrations were estimated by OD600 and verified by plate count. The initial suspension of *A. niger* was prepared as follows: 25 mL of malt extract medium (12.5%) inoculated with 2 mL of a 109 conidia/mL suspension in fresh malt extract medium previously filtered

(mycelium free), was incubated at 28°C and 150 rpm until germ tube emergence (~5 h). The inoculum was counted in a Neubauer chamber. The culture was centrifuged for 5 min at 3000g at room temperature in glass tubes (Corex). The supernatant was discarded, the pellet was re-suspended in 2 mL of minimal medium (Pontecorvo et al., 1953), and aliquoted at 0.4 mL in Eppendorf for the binding assay. The aliquots were stored at 4ºC for 24 h, and thermostatted at 28ºC for 5-10min before performing the assay.

Bacteria and yeast binding was performed according to the following technique (Cardoso, 2016). Briefly, 7 serial dilutions from an initial microorganism suspension of 0.4 mL containing 1-3x107 CFU/mL in phosphate buffer 14 mM pH 7.4 (buffer A) were done with NaCl 0.9 % (n=3). Each dilution was added with 0.8 mL of buffer E (1vol. 0.1% Tween 80 in buffer A, 1 vol. 0.04% acetic acid). After 15 min at 4°C, an aliquot of 0.1 mL complex (~740 KBq) was added to each tube and incubated for 1 h at 4°C. The entire series was assessed for radioactivity and centrifuged at 13800 g for 5 minutes at 4°C. The supernatant was discarded, the pellet re-suspended with 1 mL of solution E, and centrifuged again at 13800 g for 5 minutes at 4°C. The supernatant was carefully discarded avoiding disturbing the pellet; its final activity was measured. The binding percentage was calculated as:

$$(Net\ Pellet.act/Net\ Total.act)\ x100.$$

Being total activity ($supernatant+pellet$) (n=3)

In order to assess the binding specificity of the complex to the m.o, a competition binding assay was carried out. Each culture was pre-incubation with a solution of 10-fold molar excess of the non-radiolabelled EcgDf21-HYNIC as competitor during 1h, after that the binding assay was performed as previously described.

***In vivo* evaluation**

All biological studies were performed in compliance with the national laws of animal experimentation and approved by the Ethics Committee of the Faculty of Chemistry (N° Protocol 101900-000629-14), Universidad de la República, Uruguay. Biological evaluation was conducted in Balb C female mice, 12-14 weeks old, weighing between 25±2 g (n=3). Five groups of animals were assessed as follows: G0 = sham, G1 = sterile inflammation, G2 = *C. albicans* infection, G3 = *A. niger* infection, and G4 =. *S. aureus*. Injury induction involved subcutaneous injection in the left foreleg according to the conditions described below:

- Group 1: Sterile inflammation induced with 100 µL 1x109 Lipopolysaccharides (LPS) suspension in NaCl 0.9 % 72 hours before biodistribution studies. (Fernández, 2017)
- Group 2: Fungal infection induced with 100 µL *C. albicans* 1×109 CFU fresh culture, 72 hours before biodistribution studies
- Group 3: Fungal infection induced with 100 µL *A. niger* 1×109 CFU fresh culture (in conidia phase) 7 days before biodistribution studies
- Group 4: Bacterial infection induced with 100 µL *S. aureus* 1×109 CFU fresh culture, 72 hours before biodistribution studies.

Mice were maintained in hygienic housing conditions, with cycles of 12/12 light / dark hours and temperature of 22 ± 2°C, with food and water ad libitum.

The biodistributions were performed with [^{99m}Tc]Tc-HYNIC-EcgDf21, diluted in saline solution, it was injected into lateral tail vein (0.1 mL with a maximum activity of 1.11 MBq (30µCi), and its biodistribution was studied at 2 hours post injection. Animals were sacrificed by cervical dislocation and the organs of interest were removed, and urine, blood, muscle, and bone samples were also collected. Results were expressed as percentage dose per gram of tissue. Ratio lesion/muscle (L/M) were calculated.

Image acquisition was performed 2 hours post injection, animals were anaesthetized with 2.5% isoflurane flow 1.5-2.0 mL/min on O2. Scintigraphies were acquired in a SPECT/CT camera (NanoScan, Mediso). Reconstruction was performed with the OSEM iterative method. Analysis and quantification of images were done with PMOD 3.8 software.

Acknowledgments

The authors thank CSIC for financial project 2014, ANII PEDECIBA-Química, CMNIM-Udelar for Technetium supply, CUDIM Preclinical area for images acquisition, Roberto Castro for support in microbiological studies and Carolina Brindisi for support in radiochemical assays.

Keywords: SPECT tracers • Technetium 99m • Infection • Peptides • Radiolabelling • Defensins• *Erythrina crista-galli*• *S.aureus* • *A.niger*• *C.albicans*• Ceibo.

References:

Abrams, M.J.;Juweid, M.;Ten Kate, C.I.; Schwartz,D.A.; Hauser, M.M.; Gaul, F.E.; Fuccello, A.J.; Rubin, R.H.; Strauss, H.W.; Fischman, A.J. (1990).Technetium-99m-human polyclonal IgG radiolabeled via the hydrazinonicotinamide derivative for imaging focal sites of infection in rats. J. Nucl. Med., 31, 20-22.

Akhtar, M. S., Imran, M. B., Nadeem, M. A., & Shahid, A. (2012). Antimicrobial Peptides as Infection Imaging Agents: Better Than Radiolabeled Antibiotics. International Journal of Peptides, 2012, 1–19. https://doi.org/10.1155/2012/965238

Brouwer, C., Rahman, M., & Welling, M. (2011). Discovery and development of a synthetic peptide derived from lactoferrin for clinical use. Peptides, 32(9), 1953-1963. doi: 10.1016/j.peptides.2011.07.017

Cardoso, M., Fernández, L., Tejería, E., Esperón, P., Terán, M. (2016). Evaluation of a Labelled Bacteriophage with 99mTc as a Potential Agent for Infection Diagnosis. Current Radiopharmaceuticals, 9, 137–142. https://doi.org/10.2174/1874471009666160215162023

de Oliveira Carvalho, A. and Moreira Gomes, V.(2011). Plant Defensins and Defensin-Like Peptides - Biological Activities and Biotechnological Applications. Current Pharmaceutical Design, 17(38), pp.4270-4293.

dos Santos-Silva, C.A., Zupin, L., Oliveira-Lima M, Batista Vilela L.M., Bezerra-Neto, J.P., Ribamar Ferreira-Neto J., Cavalcanti Ferreira J.D., de Oliveira-Silva R. L., de Jesús Pires, C., Figueira Aburjaile, F., Firmino de Oliveira, M., Akio Kido, E., Crovella, S. & Benko-Iseppon, A.M. (2020) Plant Antimicrobial Peptides: State of the Art, In Silico

Prediction and Perspectives in the Omics Era. Bioinformatics and Biology Insights, 14, 1–22. https://doi.org/10.1177/1177932220952739

Fernández, L.,Terán, M. (2017). Effect of Treatment with Caspofungin on the Diagnosis of Fungal Infections by Gamma Scintigraphy. Current Radiopharmaceuticals, 10, 131 – 138. https://doi.org/10.2174/1874471010666170703125709

Follacchio, G.A.; Pala, A.; Scaccianoce, S.; Monteleone, F.; Colletti, P.M.; Rubello, D.; Liberatore, M. In vivo microbial targeting of 99mTc-labeled human B-defensin-3 in a rat model of infection. Clin. Nucl. Med. 2019, 44, e602–e606.

Gandomkar, M.; Najafi, R.; Shafiei, M.; Mazidi, M.; Goudarzi, M.; Mirfallah, S.H.; Ebrahimi, F.; Heydarpor, H.R.; Abdie, N. Clinical evaluation of antimicrobial peptide [(99m)Tc/Tricine/HYNIC(0)]Ubiquicidin 29-41 as a human-specific infection imaging agent. Nucl. Med. Biol. 2009, 36, 199–205.

Goodman.; Gilman (2007). The Pharmacological Basis of Therapeutics; Laurence L. Brunton, Ed.; Mc. Graw-Hill Interamerican: Colombia,; Vol. 11, pp. 41-69

Hegedüs, N., Marx, F. (2013). Antifungal proteins: More than antimicrobials? Fungal Biology Reviews, 26, 132–145. https://doi.org/10.1016/j.fbr.2012.07.002

Ishaq, N., Bilal, M. &. Iqbal H.M.N. (2019) Medicinal Potentialities of Plant Defensins: A Review with Applied Perspectives. Medicines, 6, 2-13. https://doi.org/10.3390/medicines6010029

Jain, S. K. (2017). The Promise of Molecular Imaging in the Study and Treatment of Infectious Diseases. Molecular Imaging and Biology, 19, 341–347. https://doi.org/10.1007/s11307-017-1055-0

Kovaleva, V., Bukhteeva, I., Kit, O.Y. & Nesmelova, I.V. (2020) Plant Defensins from a Structural Perspective. International Journal of Molecular Sciences., 21, 5307-5331. https://doi.org/10.3390/ijms21155307

Lucignani, G. (2007). The many roads to infection imaging. European Journal of Nuclear Medicine and Molecular Imaging, 34, 1873–1877. https://doi.org/10.1007/s00259-007-0574-3

Meléndez-Alafort, L., Nadali, A., Pasut, G., Zangoni, E., de Caro, R., Cariolato, L.,... Mazzi, U. (2009). Detection of sites of infection in mice using ^{99m}Tc-labeled PN2S-PEG conjugated to UBI and ^{99m}Tc-UBI: a comparative biodistribution study. Nuclear Medicine and Biology, 36, 57–64. https://doi.org/10.1016/j.nucmedbio.2008.10.011

Ordonez, A. A., Sellmyer, M. A., Gowrishankar, G., Ruiz-Bedoya, C. A., Tucker, E. W., Palestro, C. J.,... Jain, S. K. (2019). Molecular imaging of bacterial infections: Overcoming the barriers to clinical translation. Science Translational Medicine, 11(508). https://doi.org/10.1126/scitranslmed.aax8251

Padovan, L., Scocchi, M., & Tossi, A. (2010). Structural Aspects of Plant Antimicrobial Peptides. Current Protein & Peptide Science, 11, 210–219. https://doi.org/10.2174/138920310791112093

Pontecorvo.G, J.A. Roper, L.M. Chemmons, K.D. Macdonald, A.W.J. Bufton, (1953). The Genetics of Aspergillus nidulans, Editor(s): M. Demerec, Advances in Genetics, Academic Press, Volume 5,, Pages 141-238,ISSN 0065-2660, ISBN 9780120176052, https://doi.org/10.1016/S0065-2660(08)60408-3.

Reyes, A., Fernandez, L., Rey, A., Teran, M. (2014). Development and Evaluation of 99mTc-Tricarbonyl-Caspofungin as Potential Diagnostic Agent of Fungal Infections. Current Radiopharmaceuticals, 7, 144–150. https://doi.org/10.2174/1874471007666141015121838

Terán, M. A., Martínez, E., Reyes, A. L., Paolino, A., Vital, M., Esperón, P., Pacheco, J. P., Savio, E. (2011). Biological studies in animal models using [^{99m}Tc](CO)$_3$ recombinant annexin V as diagnostic agent of apoptotic processes. Nuclear Medicine and Biology, 38, 279–285. https://doi.org/10.1016/j.nucmedbio.2010.08.007

Rodriguez-Decuadro,S, Dans, P.D., Borba, M.A., Benko-Iseppon A.M., Cecchetto, G. (2019). Gene isolation and structural characterization of a legume tree defensin with a broad spectrum of antimicrobial activity, Planta. 250, 1757–1772. https://doi.org/10.1007/s00425-019-03260-w.

Signore, A., Artiko, V., Conserva, M., Ferro-Flores, G., Welling, M. M., Jain, S. K., Hess, S., & Sathekge, M. (2020). Imaging Bacteria with Radiolabelled Probes: Is It Feasible? Journal of Clinical Medicine, 9, 2372. https://doi.org/10.3390/jcm9082372

Signore, A., D'Alessandria, C., Lazzeri, E., & Dierckx, R. (2008). Can we produce an image of bacteria with radiopharmaceuticals? European Journal of Nuclear Medicine and Molecular Imaging, 35, 1051–1055. https://doi.org/10.1007/s00259-008-0762-9

Tehrani, M, Erfani, M, Amirmozafari, N (2021). [^{99m}Tc-HYNIC/EDDA]-MccJ25 antimicrobial peptide analog as a potential radiotracer for detection of infection. Chem Biol Drug Des.; 97: 904– 913. https://doi.org/10.1111/cbdd.13817

Terán, M.; Paolino, A.; Pérez Sartori, G.; Vilar, J.; Kapitan, M.; Hermida, J.C.; Andruskevicius, P.;Savio Larriera.E (2010). Evaluation of ^{99m}Tc-HYNIC-IgG for the diagnosis of infection focuses in HIV positive patients. Rev. Panam. Infectol, 12(2), 12–17.

Thevissen, K., de Mello Tavares, P., Xu, D., Blankenship, J., Vandenbosch, D., Idkowiak-Baldys, J., Govaert, G., Bink, A., Rozental, S., de Groot, P. W. J., Davis, T. R., Kumamoto, C. A., Vargas, G., Nimrichter, L., Coenye, T., Mitchell, A., Roemer, T., Hannun, Y. A., & Cammue, B. P. A. (2012). The plant defensin RsAFP2 induces cell wall stress, septin mislocalization and accumulation of ceramides in Candida albicans. Molecular Microbiology, 84(1), 166–180. https://doi.org/10.1111/j.1365-2958.2012.08017.x

Thevissen, K., Warnecke, D. C., François, I. E., Leipelt, M., Heinz, E., Ott, C., Zähringer, U., Thomma, B. P., Ferket, K. K., & Cammue, B. P. (2004). Defensins from Insects and Plants Interact with Fungal Glucosylceramides. Journal of Biological Chemistry, 279(6), 3900–3905. https://doi.org/10.1074/jbc.m311165200

Thomma, B., Cammue, B., & Thevissen, K. (2002). Plant defensins. Planta, 216(2), 193–202. https://doi.org/10.1007/s00425-002-0902-6

Trejtnar, F., & Laznicek, M. (2002). Analysis of renal handling of radiopharmaceuticals. The Quarterly Journal of Nuclear Medicine and Molecular Imaging, 46, 181–194.

Retrived from https://www.minervamedica.it

Vilche, M., Reyes, A. L., Vasilskis, E., Oliver, P., Balter, H., Engler, H. (2016). ^{68}Ga-NOTA-UBI-29-41 as a PET Tracer for Detection of Bacterial Infection. Journal of Nuclear Medicine, 57, 622–627. https://doi.org/10.2967/jnumed.115.161265

Von Guggenverg, E., Behe, M, Behr, T.M, Saurer, M., Seppi, T. Decristoforo, C. (2004). ^{99m}Tc-Labeling and in Vitro and in Vivo Evaluation of HYNIC- and (Nα-His)Acetic Acid-Modified [d-Glu1]-Minigastrin. Bioconjugate Chemistry,15, 864-871. https://doi.org/10.1021/bc0300807

Welling, M. M., Visentin, R., Feitsma, H. I., Lupetti, A., Pauwels, E. K., & Nibbering, P. H. (2004). Infection detection in mice using ^{99m}Tc-labeled HYNIC and N2S2 chelate conjugated to the antimicrobial peptide UBI 29–41. Nuclear Medicine and Biology, 31, 503–509. https://doi.org/10.1016/j.nucmedbio.2003.11.009

Xiangli Liu, X., X., Testa, B. & Fahr A., (2011). Lipophilicity and Its Relationship with Passive Drug Permeation. Pharmaceutical Research, 28, 962–977. https://doi.org/10.1007/s11095-010-0303-7.

Yeaman, M. R., & Yount, N. Y. (2003). Mechanisms of Antimicrobial Peptide Action and Resistance. Pharmacological Reviews, 55(1), 27–55. https://doi.org/10.1124/pr.55.1.2

Zasloff, M. (2002). Antimicrobial peptides of multicellular organisms. Nature, 415(6870), 389–395. https://doi.org/10.1038/415389a